

TECHNICAL ADVANCE OPEN ACCESS

# Systemic and Phloem-Specific Protein Targeting by High Affinity Nanobodies Expressed From a Plant RNA Virus Vector

Angel Y. S. Chen<sup>1</sup>  | Giada Spigolon<sup>2</sup> | Lorenzo Scipioni<sup>3,4</sup> | James C. K. Ng<sup>1</sup> 

<sup>1</sup>Department of Microbiology and Plant Pathology, University of California, Riverside, California, USA | <sup>2</sup>Beckman Institute, Caltech, Pasadena, California, USA | <sup>3</sup>Laboratory for Fluorescence Dynamics, Department of Biomedical Engineering, University of California, Irvine, California, USA | <sup>4</sup>Centre de Recherches en Cancérologie de Toulouse, Toulouse, France

**Correspondence:** James C. K. Ng ([jamesng@ucr.edu](mailto:jamesng@ucr.edu))

**Received:** 20 February 2025 | **Revised:** 26 May 2025 | **Accepted:** 28 May 2025

**Funding:** This work is supported by a California Department of Food and Agriculture grant 23-0001-039-SF (SA23-6374-01).

**Keywords:**  $\alpha$ -tubulin | endoplasmic reticulum | FRET-FLIM | nanobody | phloem | tissue tropism | viral vector

## ABSTRACT

The emergence of nanobodies (Nbs) has kindled an avid interest for their use in genetic engineering and plant biotechnology. In planta expression of Nbs has relied on either stable or transient transformation approaches that are lengthy and cannot support systemic expression, respectively. In addition, there is no precedence for studies on tissue-specific expression of Nbs. To address these issues, viral vectors could be used as an alternative, but this has not been shown. Here, this proof-of-concept study establishes a platform to demonstrate the phloem-specific targeting of proteins by Nbs expressed from a citrus tristeza virus-based vector. The vector facilitates anti-green fluorescent protein (GFP) Nb production within the phloem of transgenic *Nicotiana benthamiana* plants expressing a GFP-fused endoplasmic reticulum-targeting peptide and that of a microtubule marker line expressing GFP-fused  $\alpha$ -tubulin 6. The interaction between anti-GFP Nb and the GFP-tagged peptide/protein is corroborated by both pull-down assays and fluorescence resonance energy transfer-fluorescence lifetime imaging microscopy (FRET-FLIM) measurements. This proof-of-concept platform—including validation of Nb–antigen interaction in the phloem by FRET-FLIM analysis, which has not been described in the literature—is novel for exploring Nb-mediated functions applicable to targeting or identifying phloem proteins and those co-opted into the virus infection process.

Plants play a central role in human affairs as sources of food, energy and fibre, and as platforms for diverse biotechnology applications (Jez et al. 2016; Molina-Hidalgo et al. 2021). As the demands for plant products and plant-based applications continue to soar, strategies for enhancing their performance and productivity will be needed. Essential growth and developmental activities required to support plant performance and productivity are dependent on the translocation and unimpeded distribution of a vast array of photosynthesis assimilates and essentials like sugars and amino acids through the phloem and sieve elements (Lough and Lucas 2006; Tegeder

and Hammes 2018). In addition, communication and signaling throughout the plant like those involved in defence triggered in response to microbial pathogens are associated with phloem-specific transcriptomic and proteomic changes and mediated by the trafficking of macromolecules, phytohormones and RNA via the phloem system (Ham and Lucas 2017; Kappagantu et al. 2020; Vlot et al. 2021; Lewis et al. 2022). However, research into the communication network and interactions occurring in the phloem is challenging, in part, due to the limitation in isolating phloem tissues and accessing pure phloem exudates/sap (Knoblauch et al. 2018; Jiang

This is an open access article under the terms of the [Creative Commons Attribution-NonCommercial-NoDerivs](https://creativecommons.org/licenses/by-nc-nd/4.0/) License, which permits use and distribution in any medium, provided the original work is properly cited, the use is non-commercial and no modifications or adaptations are made.

© 2025 The Author(s). *Molecular Plant Pathology* published by British Society for Plant Pathology and John Wiley & Sons Ltd.

et al. 2019; Kappagantu et al. 2020). Novel approaches that can block, interfere with, recognise or lead to the identification of components participating in the communication network and interactions (Zhang et al. 2019) are needed to help better understand phloem processes.

We report here research leading to the development of a proof-of-concept implementation for VVPN, a viral vector-based system for producing nanobodies with affinity for protein targets within plants. A nanobody (Nb) is the antigen-binding domain of a heavy chain-only antibody (Muyldermans 2021). At a relative molecular mass of 12 to 15 kDa, Nbs are 10 times smaller than conventional antibodies. With many unique properties, such as the ability to penetrate tissues well and recognise smaller targets and active sites with little cytotoxicity, enhanced heat stability, higher solubility and refolding capacities (hence, reduced liability for aggregation), and increased resistance to pH denaturation, Nbs are ideal for use in genetic engineering and biotechnology applications (Muyldermans 2021; Wang et al. 2021). A functional VVPN is useful towards the development of direct and extended applications described in the preceding paragraph. In the context of this proof-of-concept, the utility of the VVPN framework is validated through the systemic and tissue-specific production of Nbs that target an endogenously expressed, green fluorescent protein (GFP)-fused plant peptide or protein ligand (detailed below).

The production of functional Nbs for targeting proteins in plants has been demonstrated recently through stable plant transformation and transient expression approaches (Hemmer et al. 2018; Wang et al. 2021; Kourelis et al. 2023). However, time/cost trade-offs as well as other limitations such as the lack of systemic expression (e.g., in the case of transient transformation) can diminish or even override the benefits of these approaches (Abrahamian et al. 2020). VVPN is an alternative to these approaches; when used with a viral vector that exhibits tissue tropism, VVPN shines in delivering the ability to express Nbs in specific plant tissues. In this study, we describe innovations leading to the first demonstrated phloem-specific expression of Nbs by VVPN constructed using T36CA (Chen et al. 2021), an isolate of the T36 strain of citrus tristeza virus (CTV; taxonomic name: *Closterovirus tristeza*) (Walker et al. 2020), a phloem-restricted, single-stranded, positive-sense RNA virus from the family *Closteroviridae*. Taking advantage of the phloem tropism of CTV, we engineered T36CA-based vectors carrying the coding sequence of Nb specific to GFP (GFPNb) and agroinoculated them to transgenic *Nicotiana benthamiana* plant lines expressing GFP fused with a plant peptide or protein. With this system, we demonstrate the ability of the T36CA-expressed GFPNb to recognise its target in the phloem of systemic tissues by performing pull-down assays and FRET-FLIM (fluorescence resonance energy transfer-fluorescence lifetime imaging microscopy) analysis. The latter is unique not only in showing the specificity of Nb–antigen interaction in the phloem, but also the analytical value of using FRET-FLIM measurements to determine such interactions within the phloem. Unlike non-tissue-specific viral vectors, such as those engineered on tobacco mosaic virus and potato virus X platforms, the CTV vector directs phloem-specific gene expression that is retained for a significantly longer period of years during systemic infection (Dawson and Folimonova 2013; Krueger et al. 2024), making it advantageous

for studies aimed at investigating phloem-specific interactions that take place at later developmental stages of a plant.

To demonstrate the proof-of-concept of Nb–protein target interaction driven by this VVPN platform, we made three constructs using a T36CA-based vector, pT36CA-V1.5-GFP (hereafter, simplified as pV1.5-GFP) (Krueger et al. 2024), by replacing the GFP coding sequence with each of the following: (1) GFPNb-his, (2) mCH-GFPNb-his, and (3) mCH (Figure 1a). pV1.5-GFPNb-his was engineered to express a C-terminal histidine-tagged Nb specific for GFP (GFPNb) (PDB Entry ID: 30G0). pV1.5-mCH-GFPNb-his was pV1.5-GFPNb-his engineered to express an N-terminal mCherry-tagged GFPNb, while pV1.5-mCH was pV1.5 expressing mCherry. Details of the construction steps are provided in the Data S1, Figure S1 and Table S1. Each construct was individually agroinoculated into transgenic *N. benthamiana* plants expressing potyvirus HC-Pro or mgfp5-er, a GFP-fused endoplasmic reticulum-targeting peptide (line 16c) (Data S1). Six weeks post-inoculation, the systemic leaves of plants that tested positive for viral activity (Chen et al. 2021) were subjected to the analyses as detailed in the sections below.

To demonstrate the in planta production and functionality of GFPNb, immunoblot analyses (using anti-His and anti-GFP antibodies) and pull-down assays were performed using total proteins extracted from the systemic leaves of the V1.5-GFP- or V1.5-GFPNb-his-agroinoculated plants (Data S1). As shown in Figure 1b, HC-Pro-expressing plants inoculated with V1.5-GFP accumulated GFP (lane 1). Endogenous GFP (mgfp5-er) and viral-expressed GFP were identified in V1.5-GFP-inoculated 16c plants (Figure 1b, lane 2). Both GFP species were indistinguishable from each other as they differed by only 3 kDa. Because V1.5-GFPNb-his was engineered to express GFPNb (not GFP), no GFP accumulation was observed in HC-Pro-expressing plants inoculated with V1.5-GFPNb-his (Figure 1b, lane 3). Instead, GFPNb-his was produced in V1.5-GFPNb-his-inoculated plants. GFPNb-his was also produced in 16c plants inoculated with V1.5-GFPNb-his (Figure 1b, lane 4). Together, these results indicate that V1.5-GFPNb-his is biologically active in *N. benthamiana* plants and expresses GFPNb-his. The specific binding of GFPNb-his to GFP was determined using a His-tagged protein pull-down assay. Eluted proteins from the pull-down assays were analysed by immunoblots. The anti-His antibody detected GFPNb-his in the eluate containing protein extracts of HC-Pro-expressing plants inoculated with V1.5-GFPNb-his (Figure 1b, lane 7). GFPNb-his was also detected in the eluate containing extracts of 16c plants inoculated with V1.5-GFPNb-his (Figure 1b, lane 8). In contrast, GFPNb-his was not detected in the eluate of both HC-Pro and 16c plants inoculated with V1.5-GFP (Figure 1b, lanes 5 and 6). These results indicate that the pull-down assay was successful in capturing GFPNb-his produced by V1.5-GFPNb-his. Mgfp5-er was detected in the eluate of 16c plants inoculated with V1.5-GFPNb-his (Figure 1b, lane 8) but not in 16c plants inoculated with V1.5-GFP (Figure 1b, lane 6), indicating that the interaction between GFP and GFPNb-his is highly specific.

Although the pull-down and immunoblot analyses clearly showed the specific recognition of GFPNb-his to its target antigen (GFP), it remained possible that the interactions had occurred in vitro (in the lysate) between free GFPNb-his and GFP

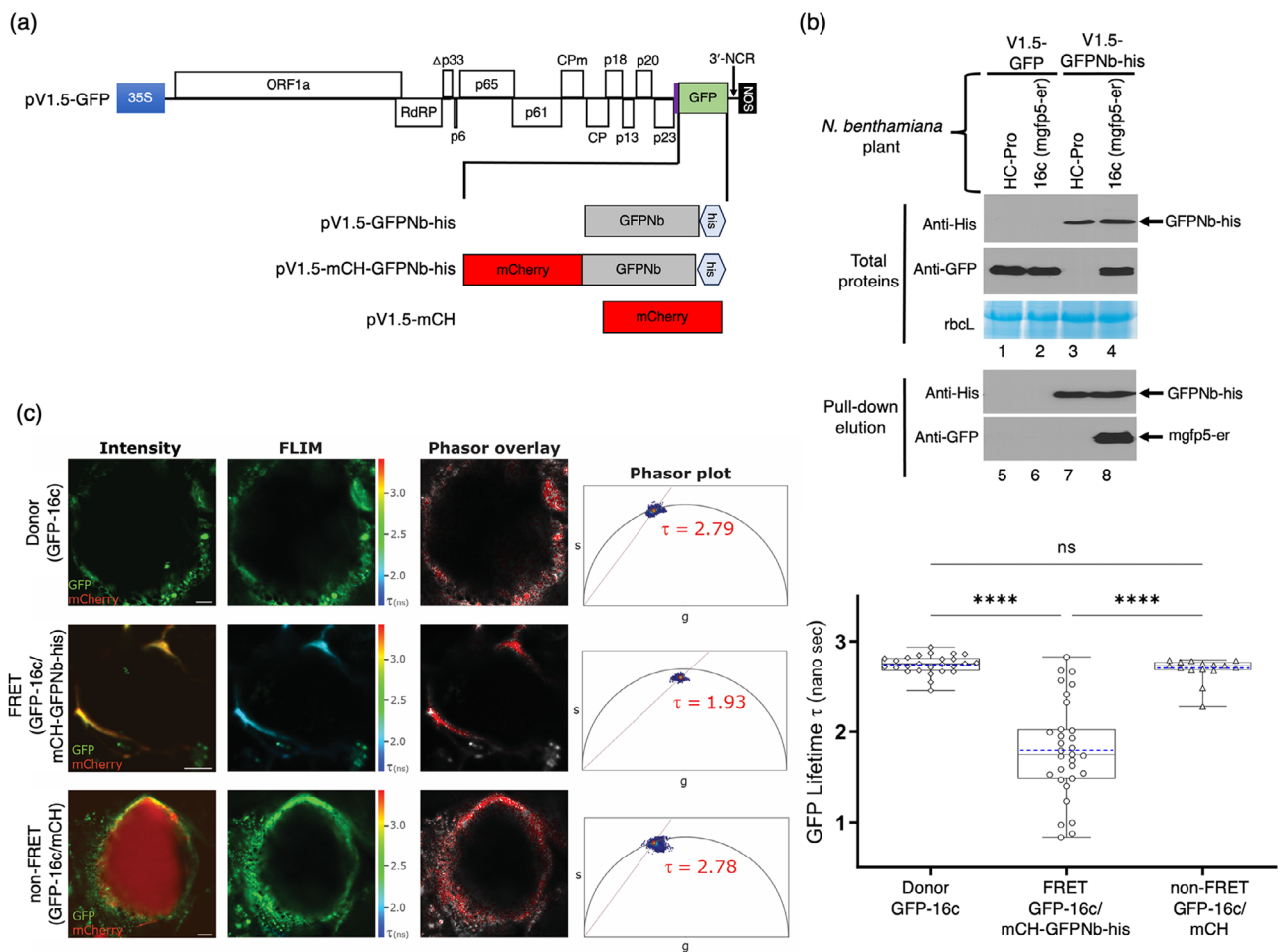


**FIGURE 1** | VVPN-mediated expression of nanobodies targeting endogenous GFP. (a) Citrus tristeza virus (CTV) T36CA-V1.5-based constructs engineered to express GFPNb-his (pV1.5-GFPNb-his), mCherry-GFPNb-his (pV1.5-mCH-GFPNb-his) or mCherry (pV1.5-mCH). 35S, cauliflower mosaic virus 35S promoter; NOS, *nopaline synthase* terminator; his, 6xhistidine tag; purple bar, CTV coat protein controller element. The genomic organisation of the vector is essentially as described in Figure S1. (b) Binding of GFPNb to its protein target in plants harbouring V1.5-GFPNb-his. Protein extracts from systemic leaves of *Nicotiana benthamiana* plants (HC-Pro or 16c) agroinoculated with the constructs (as indicated) were subjected to immunoblot analyses using anti-GFP or anti-His antibodies before (total proteins) and after His-tagged protein pull-down (pull-down elution). Coomassie blue-stained Rubisco large subunit (rbcL) served as a loading control for equal protein loading. (c) Representative FRET-FLIM measurements. The intensity panels contain dual-channels (GFP/mCherry) confocal images of phloem cells in the leaf petioles of donor-only, FRET pair and non-FRET pair samples as indicated (scale bar = 5  $\mu$ m). The FLIM panels show colour-coded maps of fluorescent lifetimes ( $\tau$ ) in the same cells, with green and blue representing longer and shorter  $\tau$ , respectively. The phasor overlay panels display (in red) the pixels that fall within the red circle in the corresponding phasor plots on the right. Clusters in the phasor plots represent the  $\tau$  values calculated from regions of interest (ROIs) in the corresponding FLIM panels. The  $\tau$  values shown in the phasor plots refer to the central value of the red circle, where most of the ROIs' pixels are mapped. The mean (blue dash line), median (solid line), as well as min and max  $\tau$  values of GFP calculated from multiple ROIs in the donor, FRET and non-FRET samples are shown in the box-and-whisker plot (\*\*\*\* $p < 0.0001$ ; ns denotes not significant).

molecules after the protein extraction process (Strotmann and Stahl 2022). To rule out this possibility, we performed confocal microscopy and FRET-FLIM experiments to determine the spatial interaction between GFP (donor) and mCH-GFPNb-his (acceptor) within the phloem of systemic (upper non-inoculated) leaf petioles of 16c plants 6 weeks post-inoculation (Data S1, Figure S2a). FRET occurs when excited-state energy from a fluorophore (the donor) is transferred to another fluorophore (the acceptor), which subsequently emits fluorescence in place of the donor. The energy transfer is highly dependent on the donor-acceptor distance ( $r^4$ , with  $r$  being the donor-acceptor distance) and possible only at a very short  $r$  value (typically below 10 nm). As such, FRET can be used to interrogate the interaction between two distinct moieties by tethering one of them to a

donor and the other to an acceptor. The presence of FRET can be detected and quantified using several methods, one of which is the measurement of the donor's shortened fluorescence lifetime. Although the FRET-FLIM approach has been used to test the binding affinity between interacting partners within plant cells (Bücherl et al. 2014), this is the first reported results of the FRET-FLIM measurements of a Nb-antigen interaction in phloem tissues. Phasor analysis was chosen as it offers a computationally straightforward and robust method for examining variations in fluorescence lifetime measurements (Digman et al. 2008). Based on this method, single exponential lifetimes such as those from only-donor populations would fall on the universal circle line, while multi-exponential lifetimes such as those related to acceptor-mediated donor quenching are found

inside the universal circle. Accordingly, as shown in Figure 1c, phasor plots from GFP-positive regions of interest (ROIs) in the phloem cells of the systemic leaf petioles of 16c plants (GFP-16c)

showed a cluster of lifetimes localised on the universal circle; the corresponding donor mean lifetime was  $\tau = 2.743$  nanosec (ns)  $\pm 0.1054$  ( $n = 26$ ). Phasor plots from GFP/mCherry ROIs

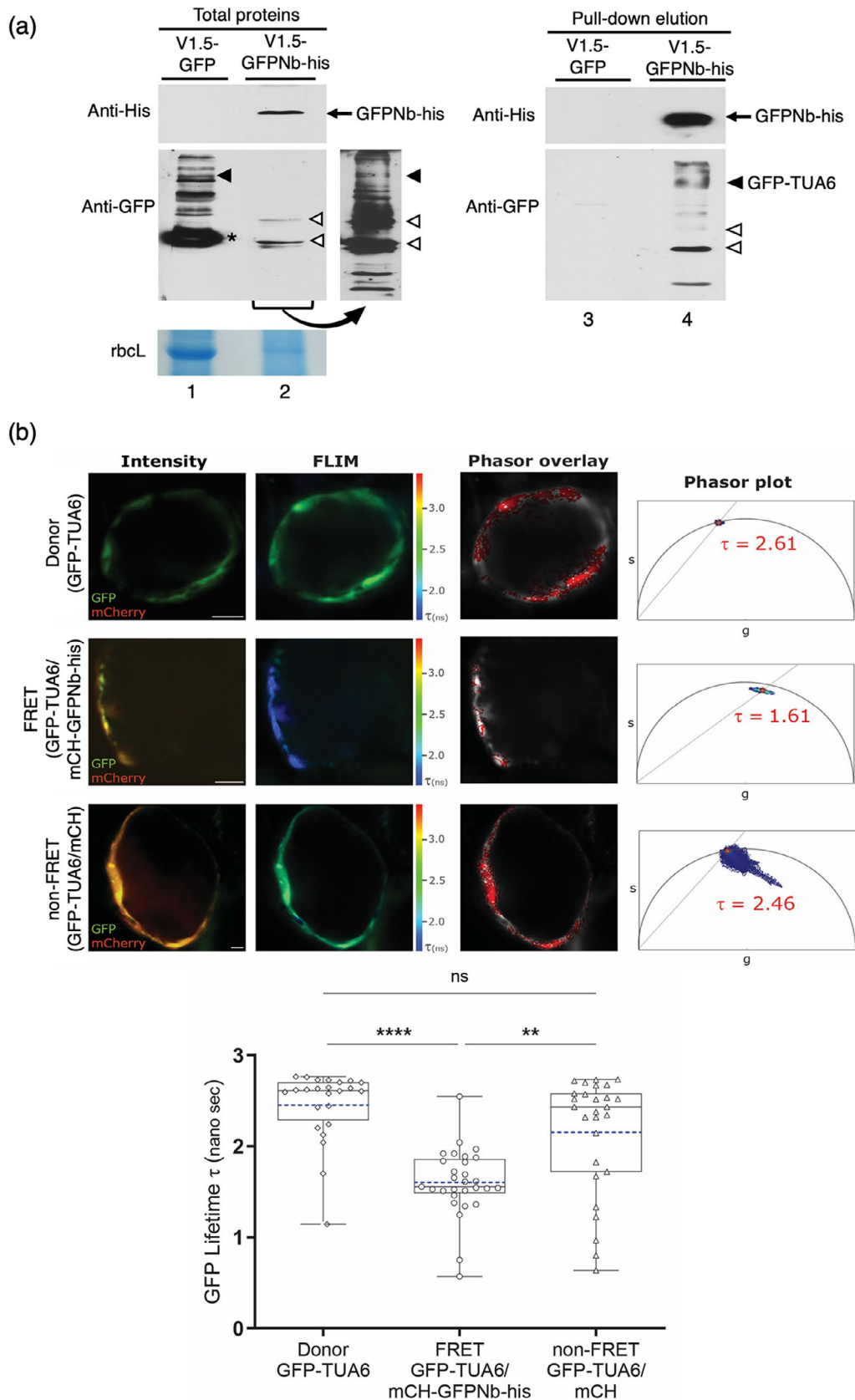


FIGURE 2 | Legend on next page.

**FIGURE 2** | In planta VVPN-mediated production of nanobodies targeting endogenous GFP fused with  $\alpha$ -tubulin (GFP-TUA6). (a) Pull-down assay to determine the binding of GFPNb to its protein target in transgenic *Nicotiana benthamiana* plants expressing GFP-TUA6. Proteins from the systemic leaves of GFP-TUA6-expressing plants agroinoculated with V1.5-GFP or V1.5-GFPNb-his were subjected to immunoblot analysis using anti-GFP or anti-His antibodies before (total proteins; left panel) and after His-tagged protein pull-down (right panel). Anti-His antibody identified the 15-kDa GFPNb-his protein (black straight arrows). Anti-GFP antibodies identified proteins with molecular masses equivalent to those of full-length (76 kDa; black triangles), truncated (white triangles) or multimeric forms of GFP-TUA6, as well as the viral-expressed GFP (27 kDa; asterisk). The curve arrow at the bottom of the immunoblot in the left panel points to an image of lane 2 following extended exposure. Equal amounts of quantified total proteins of the V1.5-GFP- and V1.5-GFPNb-his-inoculated samples were used for immunoblot analysis, but this was not reflected by the intensity of the Coomassie blue-stained Rubisco large subunit (rbcL) of the two samples. (b) FRET-FLIM measurements. The intensity panels contain dual-channels (GFP/mCherry) confocal images of phloem cells in the leaf petioles of donor-only, FRET pair and non-FRET pair samples as indicated (scale bar = 5  $\mu$ m). The FLIM panels show colour-coded maps of fluorescent lifetimes ( $\tau$ ) in the same cells, with green and blue representing longer and shorter  $\tau$ , respectively. The phasor overlay panels display (in red) the pixels that fall within the red circle in the corresponding phasor plots on the right. Clusters in the phasor plots represent the  $\tau$  values calculated from regions of interest (ROIs) in the corresponding FLIM panels. The  $\tau$  values shown in the phasor plots refer to the central value of the red circle, where most of the ROIs' pixels are mapped. The mean (blue dash line), median (solid line), as well as min and max  $\tau$  values of GFP calculated from multiple ROIs in the donor, FRET and non-FRET samples are shown in the box-and-whisker plot (\*\*\*\* $p < 0.0001$ ; \*\* $p = 0.0013$ ; ns denotes not significant).

in the phloem cells of GFP-16c/mCH-GFPNb-his (V1.5-mCH-GFPNb-his-inoculated) samples showed that the cluster of lifetimes localised inside the universal circle; the measured mean donor lifetime was  $\tau = 1.802 \text{ ns} \pm 0.5330$  ( $n = 31$ ). Phloem cells from GFP-16c/mCH (V1.5-mCH-inoculated) samples were used as non-FRETing negative control ( $\tau = 2.687 \text{ ns} \pm 0.1357$ ;  $n = 15$ ). The reduction of the donor lifetime from 2.743 to 1.802 ns detected in the GFP-16c/mCH-GFPNb-his samples indicated that GFP and the GFPNb were physically interacting. Kruskal-Wallis test ( $p < 0.0001$ ;  $H = 43.4$ ) followed by Dunn's multiple comparison showed that the difference between the donor lifetime of GFP-16c versus GFP-16c/mCH-GFPNb-his was significant ( $p < 0.0001$ ), as was the donor lifetime of GFP-16c/mCH-GFPNb-his versus GFP-16c/mCH ( $p < 0.0001$ ). In contrast, the donor lifetime of GFP-16c and GFP-16c/mCH was not significantly different ( $p > 0.999$ ).

Additional pull-down and FRET-FLIM data validating the interaction between GFPNb and GFP were obtained using samples of *N. benthamiana* microtubule marker line expressing GFP-fused  $\alpha$ -tubulin 6 (GFP-TUA6) inoculated with V1.5-GFPNb-his and V1.5-mCH-GFPNb-his, respectively. As shown in Figure 2a, proteins from the upper non-inoculated leaves of V1.5-GFP- or V1.5-GFPNb-his-inoculated GFP-TUA6 plants were subjected to immunoblot analysis before (left panel) and after His-tagged protein pull-down (right panel). GFPNb-his was not detected by anti-His antibodies in the protein extracts of plants inoculated with V1.5-GFP (lane 1), but was identified in those inoculated with V1.5-GFPNb-his (lane 2). Following the pull-down, GFPNb-his was not detected in the eluate of the V1.5-GFP sample (lane 3) but was identified in the V1.5-GFPNb-his sample (lane 4). Anti-GFP antibodies detected full-length GFP-TUA6 (76-kDa) and the viral-expressed GFP in the total protein extracts of V1.5-GFP-inoculated plants (lane 1), but not in the pull-down eluate (lane 3). Anti-GFP antibodies also identified full-length GFP-TUA6 in the total protein extracts and pull-down eluate of the V1.5-GFPNb-his sample (lanes 2 and 4). Multiple proteins with sizes that were either smaller or bigger than that of full-length GFP-TUA6 were recognised by the anti-GFP antibodies in both the total proteins and pull-down eluate of the V1.5-GFPNb-his sample (lanes 2 and 4). Similarly sized proteins were also seen in the V1.5-GFP sample (lane 1). The identification of these proteins suggested

the presence of truncated and multimeric forms of GFP-TUA6 in GFP-TUA6-expressing *N. benthamiana* plants. Interestingly, although equal amounts of quantified total proteins were used for the pull-downs, both the Rubisco large (Figure 2a, left panel) and small (not shown) subunits (used as loading controls) were consistently more abundant in the extracts of GFP-TUA6 plants inoculated with V1.5-GFP (lane 1; negative control) than those inoculated with V1.5-GFPNb-his (lane 2). This suggested that more Rubisco degradation had occurred in plants inoculated with V1.5-GFPNb-his than those inoculated with V1.5-GFP. The basis for this occurrence is unclear. It is possible that the binding of GFP Nbs to GFP-TUA6 could have affected some aspects of microtubule functions that are tied to the regulation of specific cellular processes. Studies of Nb-antigen interactions in plants have found that Nb-bound antigens exhibit altered functions (Hemmer et al. 2018; Wang et al. 2021), while the dysfunction of microtubules can lead to intracellular protein instability (Bounoutas et al. 2011) as well as trigger the degradation and clearance of chloroplasts by autophagy (Wang et al. 2015). Given that Rubisco plays a key role in carbon fixation during photosynthesis, which takes place in the chloroplast, this raises the prospect of a link between GFP Nb-GFP-TUA6 interaction-mediated impact(s) on microtubule functions and the degradation of Rubisco observed in Figure 2a. This observation also hints at the possibility that, in plants, proteins that contribute to the processes mediated by molecules targeted by Nbs may undergo degradation and clearance. What is certain is the interaction between GFPNb-his and GFP in GFP-TUA6-expressing plants as seen in the pull-down assay (lane 4), and this is consistent with that observed in Figure 1b. Furthermore, the interaction between mCH-GFPNb-his and GFP-TUA6 in the phloem (Figure S2b) was supported by the FRET-FLIM results (being essentially similar to those obtained using 16c plants), with mean donor (GFP-TUA6), FRET (GFP-TUA6/mCH-GFPNb-his) and non-FRETing (GFP-TUA6/mCH) lifetimes of  $\tau = 2.458 \text{ ns} \pm 0.3875$  ( $n = 24$ ),  $\tau = 1.603 \text{ ns} \pm 0.3717$  ( $n = 29$ ) and  $\tau = 2.149 \text{ ns} \pm 0.6399$  ( $n = 27$ ), respectively (Figure 2b).

With the proof-of-concept here presented, we conclude that VVPN is well placed in the plant patho-biotechnology's stage to deliver operations where time-, yield- and tissue-specific dependent production of Nbs are a crucial consideration. In addition, the demonstration of VVPN opens the possibility

of using it as a platform to facilitate studies on protein trafficking, protein–protein interactions and applications aimed at improving the biological functions of plants. A vector that expresses Nbs specifically in the phloem will also be useful in unique applications that require the targeting of ubiquitously expressed proteins to be restricted to phloem tissues. One caveat to using a VVPN platform is that the intracellular environment may undergo changes upon virus infection (Kappagantu et al. 2020; Aknadibossian et al. 2023), thereby potentially offsetting the dynamics of Nb–protein target interaction as well as that of host proteins that are in close proximity to the interaction. Nevertheless, our results showed that Nb–antigen interaction driven by the CTV-based VVPN is stable, thus making it suitable for use with investigations that are aimed at identifying host proteins co-opted into the virus infection process (Zhang et al. 2019).

---

### Acknowledgements

We thank Jaclyn Zhou and Karen Xu for assistance with statistical analysis and Andres Collazo for helpful discussion. This work is supported by a California Department of Food and Agriculture grant 23-0001-039-SF (SA23-6374-01).

### Conflicts of Interest

The authors declare no conflicts of interest.

### Data Availability Statement

The data that supports the findings of this study are available in the [Supporting Information](#).

### References

- Abrahamian, P., R. W. Hammond, and J. Hammond. 2020. “Plant Virus-Derived Vectors: Applications in Agricultural and Medical Biotechnology.” *Annual Review of Virology* 7: 513–535.
- Aknadibossian, V., J. C. Huguet-Tapia, V. Golyaev, M. M. Pooggin, and S. Y. Folimonova. 2023. “Transcriptomic Alterations in the Sweet Orange Vasculature Correlate With Growth Repression Induced by a Variant of Citrus Tristeza Virus.” *Frontiers in Microbiology* 14: 1162613.
- Bounoutas, A., J. Kratz, L. Emtage, C. Ma, K. C. Nguyen, and M. Chalfie. 2011. “Microtubule Depolymerization in *Caenorhabditis elegans* Touch Receptor Neurons Reduces Gene Expression Through a p38 MAPK Pathway.” *Proceedings of the National Academy of Sciences of the United States of America* 108: 3982–3987.
- Bücherl, C. A., A. Bader, A. H. Westphal, S. P. Laptinok, and J. W. Borst. 2014. “FRET-FLIM Applications in Plant Systems.” *Protoplasma* 251: 383–394.
- Chen, A. Y. S., J. H. C. Peng, M. Polek, et al. 2021. “Comparative Analysis Identifies Amino Acids Critical for Citrus Tristeza Virus (T36CA) Encoded Proteins Involved in Suppression of RNA Silencing and Differential Systemic Infection in Two Plant Species.” *Molecular Plant Pathology* 22: 64–76.
- Dawson, W. O., and S. Y. Folimonova. 2013. “Virus-Based Transient Expression Vectors for Woody Crops: A New Frontier for Vector Design and Use.” *Annual Review of Phytopathology* 51: 321–337.
- Digman, M. A., V. R. Caiolfa, M. Zamai, and E. Gratton. 2008. “The Phasor Approach to Fluorescence Lifetime Imaging Analysis.” *Biophysical Journal* 94: L14–L16.

Ham, B. K., and W. J. Lucas. 2017. “Phloem-Mobile RNAs as Systemic Signaling Agents.” *Annual Review of Plant Biology* 68: 173–195.

Hemmer, C., S. Djennane, L. Ackerer, et al. 2018. “Nanobody-Mediated Resistance to Grapevine Fanleaf Virus in Plants.” *Plant Biotechnology Journal* 16: 660–671.

Jez, J. M., S. G. Lee, and A. M. Shero. 2016. “The Next Green Movement: Plant Biology for the Environment and Sustainability.” *Science* 353: 1241–1244.

Jiang, Y., C. X. Zhang, R. Chen, and S. Y. He. 2019. “Challenging Battles of Plants With Phloem-Feeding Insects and Prokaryotic Pathogens.” *Proceedings of the National Academy of Sciences of the United States of America* 116: 23390–23397.

Kappagantu, M., T. D. Collum, C. Dardick, and J. N. Culver. 2020. “Viral Hacks of the Plant Vasculature: The Role of Phloem Alterations in Systemic Virus Infection.” *Annual Review of Virology* 7: 351–370.

Knoblauch, M., W. S. Peters, K. Bell, T. J. Ross-Elliott, and K. J. Oparka. 2018. “Sieve-Element Differentiation and Phloem Sap Contamination.” *Current Opinion in Plant Biology* 43: 43–49.

Kourelis, J., C. Marchal, A. Posbeyikian, A. Harant, and S. Kamoun. 2023. “NLR Immune Receptor-Nanobody Fusions Confer Plant Disease Resistance.” *Science* 379: 934–939.

Krueger, R. R., A. Y. S. Chen, J. S. Zhou, S. Liu, H. K. Xu, and J. C. K. Ng. 2024. “An Engineered Citrus Tristeza Virus (T36CA)-Based Vector Induces Gene-Specific RNA Silencing and Is Graft Transmissible to Commercial Citrus Varieties.” *Phytopathology* 114: 2453–2462.

Lewis, J. D., M. Knoblauch, and R. Turgeon. 2022. “The Phloem as an Arena for Plant Pathogens.” *Annual Review of Phytopathology* 60: 77–96.

Lough, T. J., and W. J. Lucas. 2006. “Integrative Plant Biology: Role of Phloem Long-Distance Macromolecular Trafficking.” *Annual Review of Plant Biology* 57: 203–232.

Molina-Hidalgo, F. J., M. Vazquez-Vilar, L. D’Andrea, et al. 2021. “Engineering Metabolism in *Nicotiana* Species: A Promising Future.” *Trends in Biotechnology* 39: 901–913.

Muyldermans, S. 2021. “Applications of Nanobodies.” *Annual Review of Animal Biosciences* 9: 401–421.

Strotmann, V. I., and Y. Stahl. 2022. “Visualization of In Vivo Protein–Protein Interactions in Plants.” *Journal of Experimental Botany* 73: 3866–3880.

Tegeer, M., and U. Z. Hammes. 2018. “The Way Out and In: Phloem Loading and Unloading of Amino Acids.” *Current Opinion in Plant Biology* 43: 16–21.

Vlot, A. C., J. H. Sales, M. Lenk, et al. 2021. “Systemic Propagation of Immunity in Plants.” *New Phytologist* 229: 1234–1250.

Walker, P. J., S. G. Siddell, E. J. Lefkowitz, et al. 2020. “Changes to Virus Taxonomy and the Statutes Ratified by the International Committee on Taxonomy of Viruses (2020).” *Archives of Virology* 165: 2737–2748.

Wang, W., J. Yuan, and C. Jiang. 2021. “Applications of Nanobodies in Plant Science and Biotechnology.” *Plant Molecular Biology* 105: 43–53.

Wang, Y., X. Zheng, B. Yu, et al. 2015. “Disruption of Microtubules in Plants Suppresses Macroautophagy and Triggers Starch Excess-Associated Chloroplast Autophagy.” *Autophagy* 11: 2259–2274.

Zhang, Y., G. Song, N. K. Lal, et al. 2019. “TurboID-Based Proximity Labeling Reveals That UBR7 Is a Regulator of NLR Immune Receptor-Mediated Immunity.” *Nature Communications* 10: 3252.

### Supporting Information

Additional supporting information can be found online in the Supporting Information section.